The Molecular Structures of Gaseous Tetrafluorohydridophosphorane, HPF_4, and Trifluorodihydridophosphorane, H_2PF_3, as determined by Electron Diffraction

Anthony J. Downs* and G. Sean McGrady
Inorganic Chemistry Laboratory, University of Oxford, South Parks Road, Oxford OX1 3QR
Elizabeth A. Barnfield and David W. H. Rankin*
Department of Chemistry, University of Edinburgh, West Mains Road, Edinburgh EH9 3JJ

The structures of gaseous tetrafluorohydridophosphorane, HPF_4, and trifluorodihydridophosphorane, H_2PF_3, have been determined by electron diffraction. The results indicate that both molecules adopt structures based on a trigonal bipyramid centred on the phosphorus atom, with the hydrogen atoms occupying equatorial sites, in conformity with C_{2v} symmetry. Salient structural parameters (r_a) are: (*i*) for HPF_4, $r(P-F_{eq})$ 153.7(0.4), $r(P-F_{ax})$ 159.1(0.4), and $r(P-H)$ 132.4(4.6) pm; $H-P-F_{eq}$ 123.0(0.9) and $H-P-F_{ax}$ 87.8(0.2)°; (*ii*) for H_2PF_3, $r(P-F_{eq})$ 154.4(0.4), $r(P-F_{ax})$ 161.3(0.2), and $r(P-H)$ 132.2(1.1) pm; $H-P-F_{eq}$ 119.6(4.4) and $F_{eq}-P-F_{ax}$ 91.7(0.2)°. Replacement of fluorine by hydrogen thus results in unusually short P–H bonds, attenuation of the apical P–F bonds, and distortion of the PF_n fragment (n = 4 or 3) so that the apical P–F bonds are bent *towards*, while the equatorial P–F bonds in HPF_4 are bent *away from*, the hydrogen substituents.

The synthetic accessibility and comparative robustness of substituted fluorophosphoranes, X_nPF_{5-n}, have encouraged studies aimed at determining how the structures and reactivities of such compounds vary with the nature of X and the value of n.[1] The structures of the molecules $(CH_3)_nPF_{5-n}$ (n = 0—3)[2–4] and Cl_mPF_{5-m} (m = 1—5),[5] as determined by electron diffraction, have been used to test the valence-shell electron-pair repulsion (VSEPR) model,[6] with concepts such as 'apicophilicity'[7] evolving from these and related studies.

One group of phosphoranes which seems to have been neglected in structural terms comprises the hydrido derivatives H_nPF_{5-n} (n = 1—3). The three compounds HPF_4,[8,9] H_2PF_3,[8,9] and H_3PF_2[10] have all been synthesized and characterized by their vibrational and n.m.r. spectra; hence they appear to be monomeric species, in both the liquid and vapour phases. Studies have doubtless been inhibited by the limited thermal stabilities of the compounds, all of which deompose slowly at ambient temperatures, and also by their proclivity to attack Pyrex glass. The structure of HPF_4 has been investigated *via* a microwave study,[11] which confirmed the C_{2v} symmetry of the gaseous molecule but failed to provide independent or precise estimates of any dimension but the axial P–F distance. These deficiencies, allied to the anomalous properties of hydrogen as a ligand (as revealed by the interbond angles in a series of molecules like PX_3 which do not correlate with the electronegativity of X when X = H),[6] have prompted us to investigate the structures of gaseous HPF_4 and H_2PF_3 by electron diffraction. The refinement calculations have converged satisfactorily without the need for any additional constraints (based, for example, on the microwave studies of HPF_4), and we have been able to determine quite independently the structures of both molecules. The dimensions invite comparison with those of PF_5[2] and other fluorophosphoranes X_nPF_{5-n} (X = CH_3, n = 1—3;[3,4] X = Cl, n = 1—5[5]).

Experimental

Synthesis.—Tetrafluorohydridophosphorane and trifluorodihydridophosphorane were both prepared by the method described by Treichel *et al.*[8] This involved the gas-phase reaction (1) between phosphorus pentafluoride (Ozark-Mahoning Co.) and trimethylstannane, $(CH_3)_3SnH$ [derived in turn from the reduction of $(CH_3)_3SnCl$ with $LiAlH_4$ in butyl ether].[8] Since the gaseous products react slowly with Pyrex glass, it was possible to handle them only briefly in glass apparatus. The reaction was carried out in an evacuated 1-l Pyrex bulb pre-conditioned by exposure to elemental fluorine and connected to a vacuum line *via* joints lubricated with Voltalef 90 grease and greaseless stopcocks. The products were transferred at low pressure and fractionated immediately by trap-to-trap condensation, with HPF_4 condensing at 147 K and H_2PF_3 at 178 K. Any $HP(O)F_2$ formed during the manipulation of HPF_4 was trapped at 161 K. The purities of the fluorohydridophosphoranes were checked by reference to the i.r. spectra of the vapours and the ^1H and ^{19}F n.m.r. spectra of $CFCl_3$ solutions.[8,9] The products were each stored at 77 K in pre-conditioned Teflon-FEP ampoules each closed by a poly(tetrafluoroethylene) (ptfe) needle valve.

$$PF_5(g) \xrightarrow[-(CH_3)_3SnF(s)]{(CH_3)_3SnH(g)} HPF_4(g) \xrightarrow[-(CH_3)_3SnF(s)]{(CH_3)_3SnH(g)} H_2PF_3(g) \qquad (1)$$

Electron-diffraction Measurements.—Electron-scattering patterns were recorded on Kodak Electron Image plates using the Edinburgh gas diffraction apparatus.[12] Nozzle-to-plate distances were *ca.* 94 and 260 mm and the accelerating voltage was *ca.* 44 kV (electron wavelength *ca.* 5.7 pm). Each of the samples was held in its Teflon-FEP ampoule at 210 K and the vapour gained access to the nozzle of the diffraction apparatus (at room temperature) *via* a Teflon–stainless-steel pressure coupling and a stainless-steel needle valve. The precise nozzle-to-plate distances and electron wavelengths were determined from scattering patterns for benzene vapour recorded immediately before or after the sample patterns. Details are given in Table 1, together with the weighting functions used to set up the off-diagonal weight matrix, the correlation parameters, and final scale factors.

Details of the electron-scattering patterns were collected in digital form using a computer-controlled Joyce-Loebl MDM6 microdensitometer with a scanning program described elsewhere.[13] Calculations made use of the programs for data reduction[13] and least-squares refinement[14] described elsewhere, the complex scattering factors being those listed by Schäfer *et al.*[15]

Results

Structure Refinement.—On the evidence of ^{1}H, ^{19}F, and ^{31}P n.m.r. and vibrational spectra,[8,9] tetrafluorohydridophosphorane, HPF_4, and trifluorodihydridophosphorane, H_2PF_3, both appear to have molecular frameworks based on a trigonal bipyramid with equatorially sited hydrogen atoms, and which conform to C_{2v} symmetry. Such a structure has been endorsed for HPF_4 by analysis of the microwave spectra due to the gaseous HPF_4 and DPF_4 molecules.[11] Accordingly we adopted just such models as a basis for calculating electron-scattering intensities. In all, the models entailed five independent geometrical parameters for each molecule. With reference to Figure 1, these comprise a mean P–F distance, $r(\text{P–F})_{\text{mean}}$, the difference $r(\text{P–F}_{\text{ax}}) - r(\text{P–F}_{\text{eq}})$ between the axial (ax) and equatorial (eq) P–F bonds, the P–H distance, r(P–H), and two angles. With HPF_4 the two angles are those defined by $\text{F}_{\text{ax}}\text{–P–F}_{\text{ax}}$ and $\text{F}_{\text{eq}}\text{–P–F}_{\text{eq}}$; with H_2PF_3 the model is defined in terms of the angles $\text{H}_{\text{eq}}\text{–P–H}_{\text{eq}}$ and $\text{F}_{\text{ax}}\text{–P–F}_{\text{eq}}$. Such models account satisfactorily for the experimental radial-distribution curves (see Figure 2).

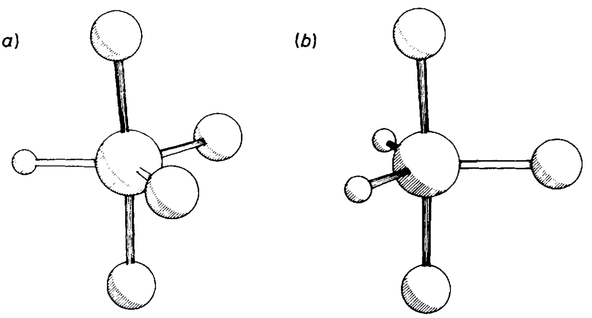

Figure 1. Perspective views of the molecules (*a*) HPF_4 and (*b*) H_2PF_3

(*a*) HPF_4. The experimental radial-distribution curve deduced from the scattering pattern of HPF_4 shows prominent, well defined peaks near 160 and 220 pm corresponding to scattering from P–F bonded and $\text{F}_{\text{ax}} \cdots \text{F}_{\text{eq}}$ non-bonded atom pairs respectively. In addition, there are weaker, more diffuse features at *ca.* 130, 260, and 320 pm which are attributable to scattering from (*i*) P–H bonded pairs, (*ii*) $\text{F}_{\text{eq}} \cdots \text{F}_{\text{eq}}$ and $\text{H} \cdots \text{F}_{\text{ax}}$ non-bonded pairs, and (*iii*) $\text{F}_{\text{ax}} \cdots \text{F}_{\text{ax}}$ non-bonded pairs respectively.

(*b*) H_2PF_3. The radial-distribution curve for H_2PF_3 is also characterized by prominent peaks near 160 and 220 pm attributable to scattering from P–F bonded and $\text{F}_{\text{ax}} \cdots \text{F}_{\text{eq}}$ non-bonded atom pairs respectively. A weaker feature at *ca.* 130 pm represents scattering from P–H bonded pairs and one at *ca.* 320 pm scattering from $\text{F}_{\text{ax}} \cdots \text{F}_{\text{ax}}$ non-bonded pairs.

Molecular scattering intensities have been calculated by established procedures, and the molecular structures have been refined on the basis of the models described by full-matrix least-squares analysis. No 'shrinkage' corrections have been applied,

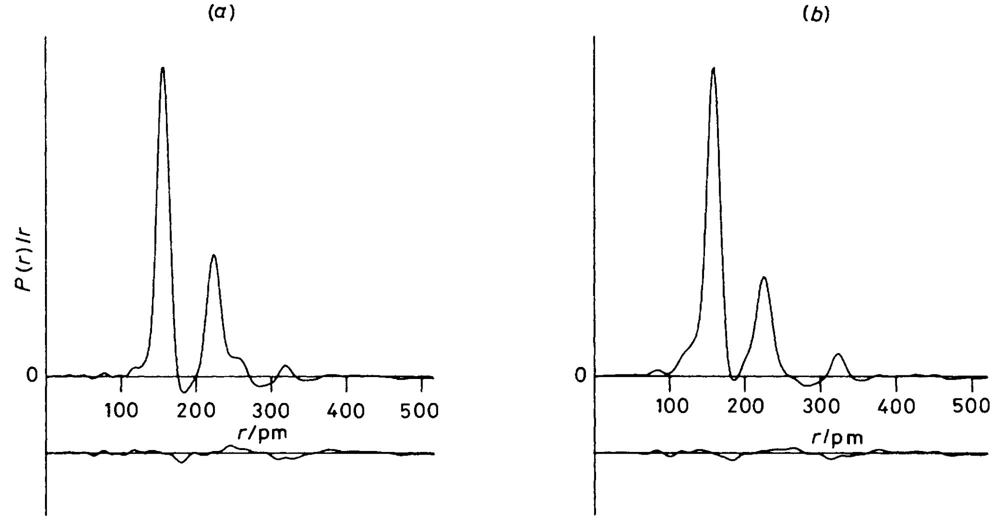

Figure 2. Observed and difference radial distribution curves, $P(r)/r$ *vs.* r, (*a*) for HPF_4 and (*b*) for H_2PF_3. Before Fourier transformation the data were multiplied by $s \cdot \exp[(-0.000\,02\,s^2)/(Z_P - f_P)(Z_F - f_F)]$

Table 1. Nozzle-to-plate distances, weighting functions, correlation parameters, scale factors, and electron wavelengths

Molecule	Nozzle-to-plate distance/mm	Δs	$s_{\text{min.}}$	sw_1	sw_2	$s_{\text{max.}}$	Correlation, p/h	Scale factor, k[a]	Electron wavelength[b]/pm
		nm^{-1}							
HPF_4	285.9	2	20	40	122	144	0.4966	0.755(12)	5.669
	128.3	4	60	80	304	356	0.4338	0.711(11)	5.666
H_2PF_3	286.0	2	20	40	122	144	0.4971	0.771(5)	5.676
	128.3	4	60	80	292	344	0.1427	0.779(10)	5.676

[a] Figures in parentheses are the estimated standard deviations of the last digits. [b] Determined by reference to the scattering pattern of benzene vapour.

Table 2. Molecular parameters for HPF_4 and H_2PF_3[a]

Parameter	HPF_4 Distance/ pm or angle/°	HPF_4 Amplitude/ pm	H_2PF_3 Distance/ pm or angle/°	H_2PF_3 Amplitude/ pm
(*a*) Independent parameters				
$r(P\text{-}F)_{mean}$	156.4(0.1)		159.0(0.1)	
$\Delta(P\text{-}F) = r(P\text{-}F_{ax}) - r(P\text{-}F_{eq})$	5.5(0.7)		6.9(0.6)	
$r(P\text{-}H)$	132.4(4.6)	8.8[b]	132.2(1.1)	10.0(1.5)
$F_{ax}\text{-}P\text{-}F_{ax}$	184.3(0.4)		183.4(0.2)[c]	
$F_{eq}\text{-}P\text{-}F_{eq}$	114.0(0.9)			
$H_{eq}\text{-}P\text{-}H_{eq}$			120.8(4.4)	
$F_{ax}\text{-}P\text{-}F_{eq}$	91.2(0.1)[c]		91.7(0.2)	
(*b*) Dependent parameters				
$r(P\text{-}F_{ax})$	159.1(0.4)	3.7(0.6)	161.3(0.2)	4.3(0.3)
$r(P\text{-}F_{eq})$	153.7(0.4)	4.0(0.6)	154.4(0.4)	5.1(0.7)
$r(F_{ax} \cdots F_{ax})$	318.1(0.7)	8.0(1.0)	322.4(0.4)	7.6(0.7)
$r(F_{eq} \cdots F_{eq})$	257.7(1.0)	8.1(1.1)		
$r(H_{eq} \cdots H_{eq})$			229.8(5.5)	12.0[b]
$r(F_{ax} \cdots F_{eq})$	223.5(0.2)	6.6(0.3)	226.5(0.2)	6.3(0.3)
$r(F_{eq} \cdots H)$	251.6(4.4)	11.0[b]	247.9(2.8)	11.0[b]
$r(F_{ax} \cdots H)$	203.2(3.0)	11.0[b]	207.0(0.7)	8.8(1.5)

[a] Figures in parentheses are the estimated standard deviations of the last digits. [b] Fixed. [c] Dependent parameter.

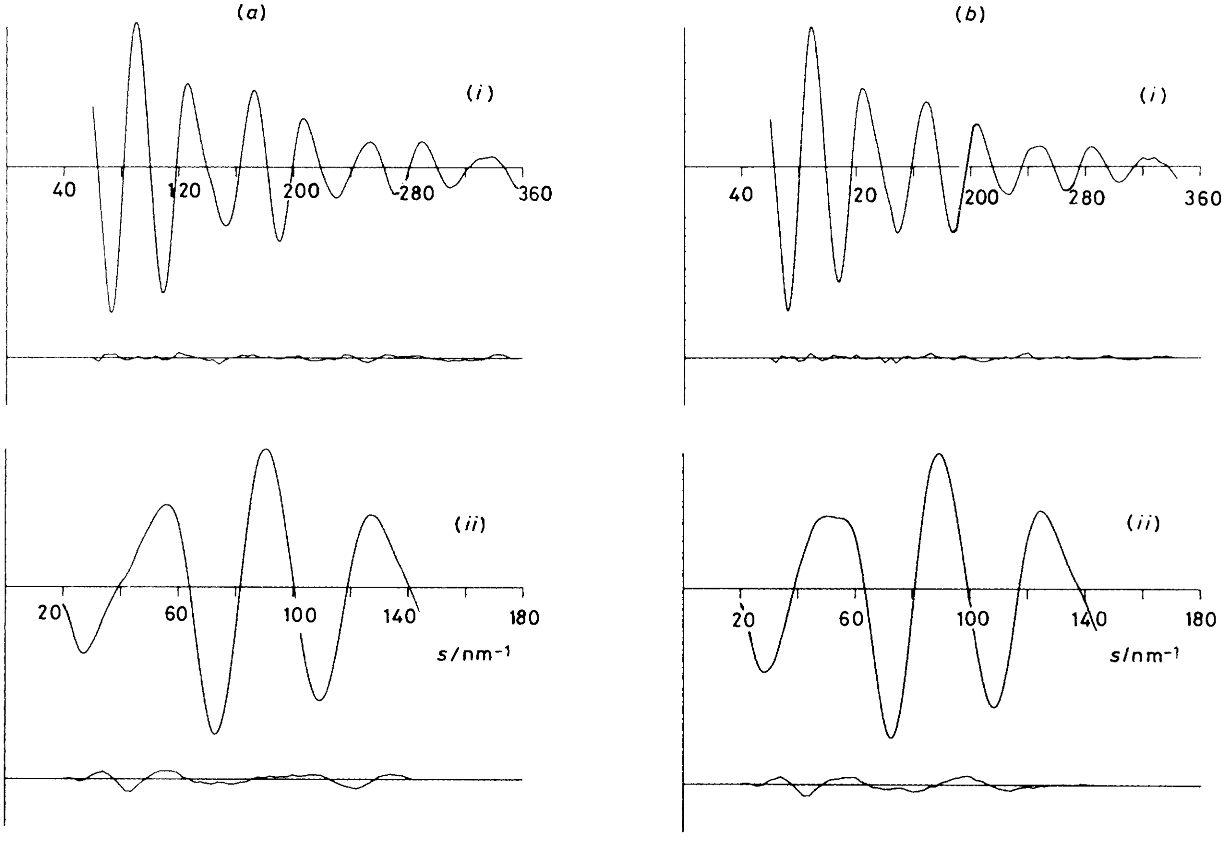

Figure 3. Experimental and final difference molecular-scattering intensity curves (*a*) for HPF_4 and (*b*) for H_2PF_3; nozzle-to-plate distance (*i*) 128.3 mm and (*ii*) 285.9 (HPF_4) or 286.0 mm (H_2PF_3)

but there is no reason to suppose that such corrections will alter significantly the results of our calculations.

All five of the independent geometrical parameters used to define each of the molecular models have yielded to simultaneous refinement. Independent refinement is also possible for five amplitudes of vibration in HPF_4 (associated with the bonded $P\text{-}F_{ax}$ and $P\text{-}F_{eq}$, and the non-bonded $F_{ax} \cdots F_{ax}$, $F_{ax} \cdots F_{eq}$, and $F_{eq} \cdots F_{eq}$ distances) and six such amplitudes in H_2PF_3 (see Table 2). Otherwise we have drawn on the precedents set by related molecules, *e.g.* PH_3,[16a] P_2H_4,[16b]

Table 3. Portions of the least-squares correlation matrices (*a*) for HPF_4 and (*b*) for H_2PF_3 showing off-diagonal elements greater than 50%

(*a*)

r(P–H)	F_{ax}–P–F_{ax}	F_{eq}–P–F_{eq}	u(P–F_{ax})	u(P–F_{eq})	k_1*	k_2*	
55	−64	−53					r(P–F)$_{mean}$
		51	−82	−73			Δ(P–F)
		−59			−57	−59	r(P–H)
						51	k_1*

(*b*)

r(P–H)	F_{ax}–P–F_{eq}	u(P–F_{eq})	u(P–F_{ax})	u($F_{ax}\cdots F_{eq}$)	k_2*	
50						r(P–F)$_{mean}$
	61	−83	−86			Δ(P–F)
					−58	r(P–H)
			−55			F_{ax}–P–F_{eq}
			76			u(P–F_{eq})
				55		u($F_{ax}\cdots$H)

* Scale factor.

Table 4. Dimensions of molecules of the type X_nPF_{5-n} (n = 0—2), where X = H, CH_3, Cl, or CF_3

Molecule	r(P–F_{eq})/pm	r(P–F_{ax})/pm	r(P–X)/pm	X_{eq}–P–X_{eq}/°	X_{eq}–P–F_{ax}/°	Ref.
PF_5	153.2(0.3)	158.0(0.2)		120[a]	90[a]	2
HPF_4	153.7(0.4)	159.1(0.4)	132.4(4.6)	114.0(0.9)[b]	87.8(0.2)[c]	This work
H_2PF_3	154.4(0.4)	161.3(0.2)	132.2(1.1)	120.8(4.4)[d]	91.7(0.1)[c]	This work
CH_3PF_4	154.3(0.4)	161.2(0.4)	178.0(0.5)	118.9(0.5)[b]	91.8(0.4)[f]	3
$(CH_3)_2PF_3$	155.3(0.6)	164.3(0.3)	179.8(0.4)	121.0(0.4)[g]	89.9(0.3)[e]	3
$ClPF_4$	153.5(0.3)	158.1(0.4)	200.0(0.3)	117.8(0.7)[b]	90.3(0.4)[e]	5
Cl_2PF_3	153.8(0.7)	159.3(0.4)	200.2(0.3)	121.8(0.4)[h]	90.0(0.3)[e]	5
CF_3PF_4[i]	153.7(0.5)	157.3(0.7)	188.1(0.8)	117.4(3.4)[b]	90[a,e]	17

[a] Not refined. [b] F_{eq}–P–F_{eq}. [c] F_{ax}–P–H_{eq}. [d] H_{eq}–P–H_{eq}. [e] F_{ax}–P–F_{eq}. [f] C_{eq}–P–F_{ax}. [g] C_{eq}–P–C_{eq}. [h] Cl_{eq}–P–Cl_{eq}. [i] Equatorial conformer.

CH_3PH_2,[16c] and S=PHF_2,[16d] to fix reasonable values for the remaining amplitudes.

The success of the refinements may be assessed from the difference between the experimental and calculated radial-distribution curves (Figure 2). Figure 3 offers a similar comparison between the experimental and calculated molecular scattering. The structural details and vibrational amplitudes of the optimum refinements, corresponding to $R_G = 0.075$ ($R_D = 0.063$) for HPF_4 and $R_G = 0.058$ ($R_D = 0.059$) for H_2PF_3, are listed in Table 2. The estimated standard deviations allow for the effects of correlation and take account of systematic errors in the electron wavelength, nozzle-to-plate distances, *etc.* Despite appreciable correlation of certain parameters, *e.g.* those defining the P–F and P–H distances (see Table 3), the main features of both structures are well defined.

Discussion

The structure of the molecule H_2PF_3 has not been determined previously and the earlier microwave study of gaseous HPF_4[11] afforded only the following parameters: r_o(P–F_{ax}) 159.4(0.5) and r_o(P–F_{eq}) 155(3) pm; H–P–F_{ax} 90(4) and H–P–F_{eq} 124(2)°. The results we have deduced from the electron-diffraction patterns are, therefore, for H_2PF_3, quite new and, for HPF_4, more extensive and better defined than (while being pleasingly consistent with) those originating in the microwave study. Our analysis confirms that gaseous HPF_4 and H_2PF_3 each adopt a structure approximating to a trigonal bipyramid; each has C_{2v} symmetry with the hydrogen atom or atoms occupying equatorial sites. This is to be expected on the basis of 'apicophilicity' arguments[7] to the effect that the apical positions are favoured by the more electronegative substituent, although the molecular structures of certain phosphoranes appear to be at odds with this principle.[17] Our results are thus amongst the few to offer a commentary on the 'apicophilicity' of hydrogen in these circumstances.

Collation of the dimensions of HPF_4 and H_2PF_3 with those of related fluorophosphoranes (Table 4) is revealing for the light it sheds on the stereochemical effects of substituting hydrogen for fluorine. Three features catch the eye.

(*i*) The P–F distances in PF_5,[2] HPF_4, and H_2PF_3 (see Table 4) reveal that successive replacement of fluorine by hydrogen in the equatorial belt of PF_5 causes extension of the remaining P–F bonds. In this respect, however, there is a striking difference between the equatorial P–F bonds, which are lengthened by only 1.2 pm, and the apical P–F bonds, which are lengthened by 3.3 pm in the switch from PF_5 to H_2PF_3. The disproportionate effect on the apical P–F bonds is apparent from the parameter

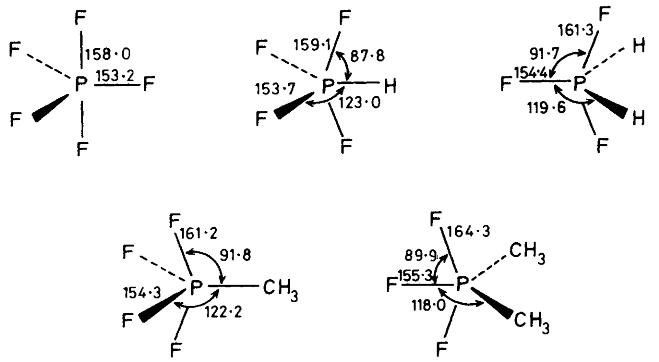

Figure 4. Structures of the molecules PF_5, HPF_4, H_2PF_3, CH_3PF_4, and $(CH_3)_2PF_3$; distances in pm, angles in °

$\Delta(P\text{–}F) = r(P\text{–}F_{ax}) - r(P\text{–}F_{eq})$ which varies from 4.8, through 5.5, to 6.9 pm in the series PF_5, HPF_4, H_2PF_3. Similar, but more pronounced, changes occur when equatorial fluorine atoms give place successively to methyl substituents, with $\Delta(P\text{–}F) =$ 4.8, 6.9, and 9.0 pm for PF_5, CH_3PF_4, and $(CH_3)_2PF_3$, respectively.[3] On the other hand, substitution of fluorine by chlorine[5] or CF_3[17] produces little or no such attenuation.

This effect can be rationalized by either VSEPR or molecular-orbital (m.o.) arguments. The VSEPR argument turns on the increased repulsion developed in the valence shell of the central phosphorus atom by the electron pair forming the bond to a less electronegative substituent like H or CH_3. The electron pairs forming the apical P–F bonds suffer a proportionately greater repulsion than those forming the equatorial P–F bonds because they come closer to the spatially more demanding P–H or P–C electron pair. Simple m.o. arguments would interpret the changes as a sign of the poorer energy match between the $3p$ orbital of the phosphorus and the $2p$ orbitals of the apical fluorine atoms; the reduced overlap which this implies is thus a consequence of the decrease in effective electronegativity at the phosphorus centre attending the replacement of fluorine by a less electronegative substituent.[18]

(*ii*) The P–H bonds in HPF_4 and H_2PF_3, at about 132 pm, are roughly 10 pm shorter than typical distances in phosphines or molecules containing four-co-ordinate phosphorus(V) centres (*cf.* PH_3 143.7,[16a] P_2H_4 145.1,[16b] CH_3PH_2 142.3,[16c] and $S{=}PF_2H$ 141.9 pm[16d]). A similar but less pronounced phenomenon is displayed by the P–C bonds which are appreciably shorter in the fluorophosphoranes CH_3PF_4 (178.0 pm) and $(CH_3)_2PF_3$ (179.8 pm) than in the parent phosphine $(CH_3)_3P$ (184.7 pm).[19]

(*iii*) The P–F bond lengths in the molecules HPF_4 and H_2PF_3 may comply with the predictions of the VSEPR model,[6] but the bond angles are another matter. The apical P–F bonds in both molecules are bent, not away from, but *towards* the equatorial P–H bonds (see Figure 4). This finding is plainly at odds with the VSEPR arguments deployed to account for the attenuation of the apical P–F bonds in the series PF_5, HPF_4, H_2PF_3. These arguments lead us to expect angular distortions of the PF_n fragments similar in sense, if not in magnitude, to those displayed in the molecules CH_3PF_4 and $(CH_3)_2PF_3$,[3] with the apical P–F bonds bent away from the less electronegative substituents. It is not possible, within the limits of experimental error, to decide whether the bond angles within the equatorial H_2PF fragment of H_2PF_3 depart significantly from the ideal values of 120°, but our analysis of HPF_4 implies that the equatorial P–F bonds of this molecule are bent *away from* the hydrogen atom. In other words, the heavy-atom framework of HPF_4 adopts a structure reminiscent of that of an SF_4-type molecule with very bulky equatorial substituents, *e.g.* $(p\text{-}CH_3C_6H_4)_2SeX_2$ (X = Cl or Br) and $(C_6H_5)_2TeBr_2$,[6] where the apical bonds are bent away from these substituents and the lone pair in the valence shell of the Group 6 atom appears not to be exerting its full stereochemical effect. The lack of both core and non-bonding valence electrons must make hydrogen an exceptional ligand in terms of its non-bonded interactions and, with respect to its nearest neighbours in the co-ordination shell of a molecule like HPF_4, the weakness of these interactions may offset the spatial demands of the P–H bonding electron pair. Yet no such arguments can reconcile the angular shapes of the molecules HPF_4 and H_2PF_3 with the progressive elongation of the apical P–F bonds in the series $PF_5 < HPF_4 < H_2PF_3$. Whatever stereochemical role may be exercised by interelectron repulsion of one sort or another, the results of our studies demonstrate that such repulsion cannot be the sole factor determining the shapes of the molecules. Attractive $H \cdots F$ interactions must be presumed also to play a role in the structures we deduce. It is somewhat ironic that another pair of fluorophosphoranes, namely CH_3PF_4 and $(CH_3)_2PF_3$, should provide the VSEPR model with one of its major triumphs,[6] when the corresponding hydrido derivatives defy the model.

The vibrational amplitudes determined independently in HPF_4 and H_2PF_3 hold no surprises. Thus they are in sensible agreement with the analogous parameters deduced for related fluorophosphoranes[2–5] and compounds containing P–H bonds on the basis of their electron-diffraction patterns or vibrational spectra.*

---

* *Note added in proof.* Very recent *ab initio* calculations on HPF_4 and H_2PF_3[20] yield bond lengths generally in good agreement with the experimental results presented here.

Acknowledgements

We thank the S.E.R.C. for the award of a research studentship (to G. S. M.), for financial support of the Edinburgh electron-diffraction service, and for provision of microdensitometer facilities.

References

1 See, for example, R. Schmutzler, in 'Halogen Chemistry,' ed. V. Gutmann, Academic Press, New York, 1967, vol. 2, p. 31.
2 K. W. Hansen and L. S. Bartell, *Inorg. Chem.*, 1965, **4**, 1775; H. Kurimura, S. Yamamoto, T. Egawa, and K. Kuchitsu, *J. Mol. Struct.*, 1986, **140**, 79.
3 L. S. Bartell and K. W. Hansen, *Inorg. Chem.*, 1965, **4**, 1777.
4 H. Yow and L. S. Bartell, *J. Mol. Struct.*, 1973, **15**, 209.
5 C. Macho, R. Minkwitz, J. Rohmann, B. Steger, V. Wolfel, and H. Oberhammer, *Inorg. Chem.*, 1986, **25**, 2828.
6 R. J. Gillespie, *Angew. Chem., Int. Ed. Engl.*, 1967, **6**, 819; 'Molecular Geometry,' van Nostrand Reinhold, London, 1972.
7 R. G. Cavell, D. D. Poulin, K. I. The, and A. J. Tomlinson, *J. Chem. Soc., Chem. Commun.*, 1974, 19; R. G. Cavell, J. A. Gibson, and K. I. The, *J. Am. Chem. Soc.*, 1977, **99**, 7841.
8 P. M. Treichel, R. A. Goodrich, and S. B. Pierce, *J. Am. Chem. Soc.*, 1967, **89**, 2017.
9 R. R. Holmes and R. N. Storey, *Inorg. Chem.*, 1966, **5**, 2146.
10 F. Seel and K. Velleman, *Z. Anorg. Allg. Chem.*, 1971, **385**, 123.
11 S. B. Pierce and C. D. Cornwell, *J. Chem. Phys.*, 1968, **48**, 2118.
12 C. M. Huntley, G. S. Laurenson, and D. W. H. Rankin, *J. Chem. Soc., Dalton Trans.*, 1980, 954.
13 S. Cradock, J. Koprowski, and D. W. H. Rankin, *J. Mol. Struct.*, 1981, **77**, 113.
14 A. S. F. Boyd, G. S. Laurenson, and D. W. H. Rankin, *J. Mol. Struct.*, 1981, **71**, 217.
15 L. Schäfer, A. C. Yates, and R. A. Bonham, *J. Chem. Phys.*, 1971, **55**, 3055.

16 (*a*) L. S. Bartell and R. C. Hirst, *J. Chem. Phys.*, 1959, **31**, 449; K. Kuchitsu, *J. Mol. Spectrosc.*, 1961, **7**, 339; (*b*) B. Beagley, A. R. Conrad, J. M. Freeman, J. J. Monaghan, B. G. Norton, and G. C. Holywell, *J. Mol. Struct.*, 1972, **11**, 371; (*c*) L. S. Bartell, *J. Chem. Phys.*, 1960, **32**, 832; (*d*) P. D. Blair, S. Cradock, and D. W. H. Rankin, *J. Chem. Soc., Dalton Trans.*, 1985, 755.

17 H. Oberhammer and J. Grobe, *Z. Naturforsch., Teil B*, 1975, **30**, 506; H. Oberhammer, J. Grobe, and D. LeVan, *Inorg. Chem.*, 1982, **21**, 275.

18 A. J. Downs, M. J. Goode, G. S. McGrady, I. A. Steer, D. W. H. Rankin, and H. E. Robertson, *J. Chem. Soc., Dalton Trans.*, 1988, 451.

19 L. S. Bartell and L. O. Brockway, *J. Chem. Phys.*, 1960, **32**, 512.

20 J. A. Deiters, R. R. Holmes, and J. M. Holmes, *J. Am. Chem. Soc.*, 1988, **110**, 7672.

Received 13*th June* 1988; *Paper* 8/02339E